International Journal of Advanced Research in Engineering Technology & Science

ISSN: 2349-2819

Email: editor@ijarets.org Volume-9, Issue-6 June – 2022 www.ijarets.org

Simulations of large and small scale features in star formation using mathematical models

Komal Gupta

M.Phil, Roll No: 150483

Session: 2015-16

University Department of Mathematics

B.R.A Bihar University, Muzzaffarpur

Abstract

As a general rule, the development of stars in the universe, particularly blue stars, is the subject of this exposition. The biggest, generally monstrous, and most brilliant stars are blue ones. The foundation and joining into a computational calculation of a direct numerical model of star development. We can become familiar with how stars foster thanks to this program. Models from both reality and fiction had been utilized to help this thought.

Keywords: *Star formation; Blue stars; Galaxy*

Introduction

The brightest stars are those that are blue. On the main sequence of the Hertsprung-Russel diagram, they were situated in the upper left. In addition to being the largest and most massive main sequence stars, these stars are also the largest. However, despite their great mass, they are unable to offset the high luminosity. This indicates that even though they have a larger supply of hydrogen than stars like the Sun, they will burn through it so quickly that their overall lifespan will be much shorter than that of medium or massive stars. Why is it crucial to keep an eye out for these transient stars? They won't have had the chance to travel very far from their birthplace because of how brief their overall lifespan will be. As a result, we must hunt for areas with bright blue stars if we wish to find galactic regions where star production is probable. This is not always possible in our own galaxy because interstellar clouds obstruct our view, but there are plenty of other galaxies to choose from. In spiral galaxies' outer regions, blue stars are bright. Due to the great brilliance of these blue stars, which makes up for their sparse quantity, the spiral components of these galaxies truly have a blue colour. The presence of extended hydrogen and dust clouds, another significant component of the spiral arms, raises the possibility that stars are formed there by gravitational collapse and condensation. Numerous images captured from deep clouds in the Galaxy clearly display protostars, which are spherical condensations. These protostars' near surroundings frequently contain young stars. The temperature of a gas cloud typically rises as a result of contraction. But in the early stages, where the temperature and pressure in the cloud remain low, the radiation can escape. As a result, the cloud will keep on collapsing and eventually split into several smaller collapsing clouds. The gravitational field is powerful enough to compensate for rising pressure by the time the central density reaches a level that renders the centre opaque to infrared radiation. It is now certain that the system will collapse, and it won't stop until the temperature inside reaches several million Kelvin. This is the minimum temperature to start the nuclear fusion of hydrogen into helium, a process that releases an enormous amount of energy. This energy is transposed through the cloud and radiated away in space. The flow of energy also restores hydrostatic equilibrium. The cloud has now become a normal core hydrogen burning star. An important amount of kinetic energy is released during the contraction stage. It is necessary for the energy to be neutralized without heating the cloud to prevent any further contraction. CO molecules play an especially important role as cooling mechanisms in the dust clouds.

Conditions of association between the parts

The three mass parts will be depicted by the variable S for the complete mass of dynamic stars, M for the all out mass of sub-atomic mists, and A for the all out mass of nuclear mists. It is accepted that the complete mass of the framework stays steady; in this manner, we expect that how much mass lost by heavenly development is precisely supplanted by new nuclear mists entering the star arrangement locale from the remainder of the World. Assuming we call the complete mass of the framework T, we might compose

$$\mathbf{T = A+M+S}$$

There are three sorts of collaboration for the nuclear cloud part A. In the first place, there is a consistent renewal by new nuclear mists in a sum equivalent to how much mass leaving the dynamic framework by heavenly development. How much new gas may thusly be considered as proprotional to how much heavenly mass S. We will call the relative steady of this cycle K1. Besides, the nuclear part is expanded as youthful, dynamic stars lose mass by heavenly breeze. This interaction is additionally corresponding to the quantity of stars and thusly to theportional to the quantity of dynamic stars currently present. Allow us to call the corresponding steady K4. This cycle expands the mass of heavenly part. Two other cycle decline it: heavenly advancement, for which we might utilize K1, and mass misfortune by heavenly breeze, for which we again use K2. The two cycles are relative to how much heavenly mass. Hence, the condition portraying the variety of heavenly mass in the framework is:

$$\frac{\mathrm{d}S}{\mathrm{d}t} = K_4 S M^n - K_1 S - K_2 S.$$

At last, the variety of the absolute sub-atomic mass is given by two cycles previously portrayed: change of nuclear into atomic gas, which increments for the variable M, and heavenly development, which diminishes how much sub-atomic mass. The condition for M will be

$$\frac{\mathrm{d}M}{\mathrm{d}t} = K_3 A M^2 - K_4 S M^n.$$

It is not difficult to see that each cycle in one of the three differential conditions is a repaid by the interaction with a contrary sign in one of different conditions. This equilibrium ensures the preservation of the aggregate sum of mass. The three free factors A, M and S in the past area are connected by the way that we think about the complete mass T of the star development framework as consistent. One may, for example, supplant S by T, A, M in Eqs. (2) and (4). The framework then, at that point, diminishes to just two first-request conditions. Moreover, it is feasible to move these two leftover conditions by presenting new layered factors and another layered time coordinate x

$$a = \frac{A}{T}$$

$$m = \frac{M}{T}$$

$$s = \frac{S}{T}$$

$$x = (K_1 + K_2)t.$$

This implies that

$$a + m + s = 1,$$

at each second. The boundaries K1; K2; K3, and K4 are likewise changed as an outcome of the layered factors and become two new boundaries

$$k_1 = \frac{K_3 T^2}{K_1 + K_2},$$

and

$$k_2 = \frac{K_4 T^n}{K_1 + K_2}.$$

At the point when two out of the three factors are known, the third additionally is known, since the amount of the three is consistently one. The differential conditions, after disposal of S and in the wake of presenting new factors, become

$$\frac{da}{dx} = 1 - a - m - k_1 m^2 a,$$

$$\frac{dm}{dx} = k_1 m^2 a + k_2 m^n (a - 1 + m).$$

These are the conditions which can be tackled. They contain three free boundaries k1; k2 and n. The outcomes may graphically be addressed in two ways. It is, obviously, conceivable to plot the three factors - the nuclear, sub-atomic, and heavenly substance - as elements of time. This is finished for various models whose results will be talked about later. One more conceivable technique frequently utilized in undeniably applied sciences is to work with stage outlines. Consider, for example, a mass holding tight a spring. The mass will bounce all over, occasionally swaying around the condition of rest. We may by and by plot the position and the speed as elements of the time in two separate drawings, yet another way is to plot the position X on the level hub and the comparing speed V on the upward pivot. We will then get a point that continuing on circle in the XV plane. On the off chance that the motions are damped, the span will gradually diminish unit the circle psychologists to a point on the X-hub. This implies that the position is steady and the speed is zero. The mass has stopped.

Star Development

Reason Registering a model of a star-shaping district with negative and positive criticism instruments, where the model incorporates three parts: cool Greetings, dust sub-atomic gas, and youthful stars with their related HII locales. Input 1. n, 2. k1 (k1), 3. k2 (k2), 4. m0 (m0), 5. s0 (s0), 6. a0 (a0). Yield one of the two unique systems that reproduce the three-parts of a star-framing district:

1-development towards a fixed state, or

2-development towards a breaking point cycle.

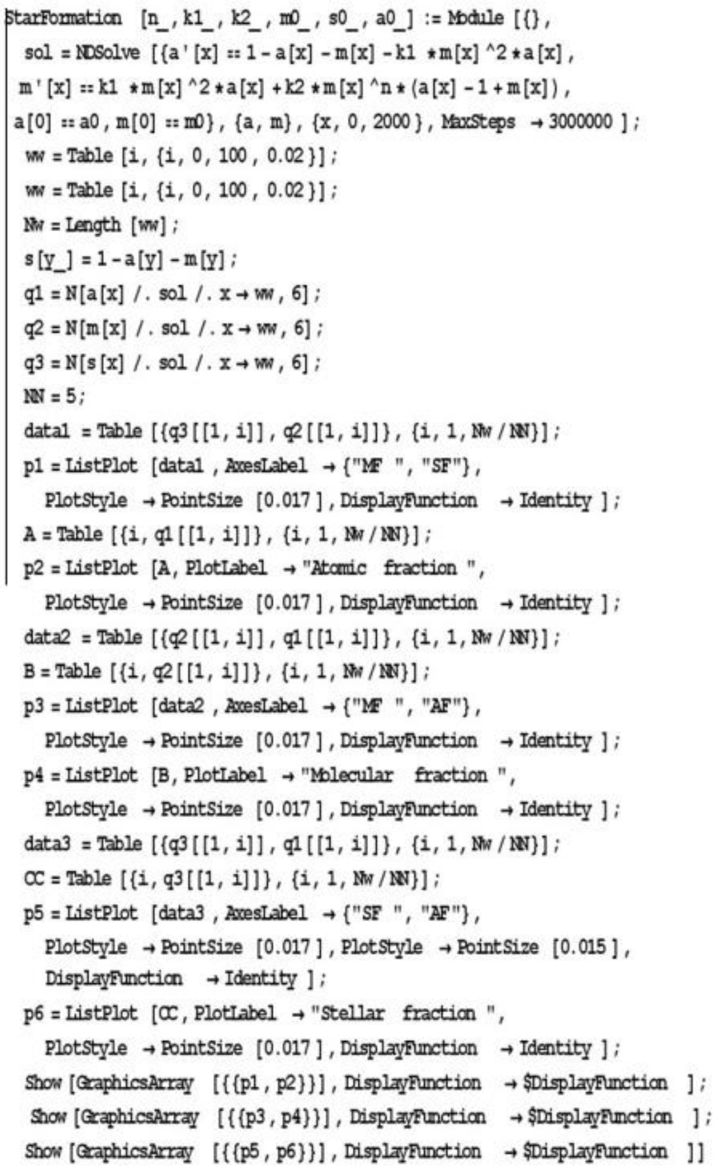

```
StarFormation [n_, k1_, k2_, m0_, s0_, a0_] := Module [{},
 sol = NDSolve [{a'[x] == 1 - a[x] - m[x] - k1 *m[x] ^2 *a[x],
 m'[x] == k1 *m[x] ^2 *a[x] + k2 *m[x] ^n * (a[x] - 1 + m[x]),
a[0] == a0, m[0] == m0}, {a, m}, {x, 0, 2000}, MaxSteps → 3000000 ];
 ww = Table [i, {i, 0, 100, 0.02}];
 ww = Table [i, {i, 0, 100, 0.02}];
 Nw = Length [ww];
 s[y_] = 1 - a[y] - m[y];
 q1 = N[a[x] /. sol /. x → ww, 6];
 q2 = N[m[x] /. sol /. x → ww, 6];
 q3 = N[s[x] /. sol /. x → ww, 6];
 NN = 5;
 data1 = Table [{q3[[1, i]], q2[[1, i]]}, {i, 1, Nw / NN}];
 p1 = ListPlot [data1, AxesLabel → {"MF ", "SF"},
   PlotStyle → PointSize [0.017 ], DisplayFunction → Identity ];
 A = Table [{i, q1[[1, i]]}, {i, 1, Nw / NN}];
 p2 = ListPlot [A, PlotLabel → "Atomic fraction ",
   PlotStyle → PointSize [0.017 ], DisplayFunction → Identity ];
 data2 = Table [{q2[[1, i]], q1[[1, i]]}, {i, 1, Nw / NN}];
 B = Table [{i, q2[[1, i]]}, {i, 1, Nw / NN}];
 p3 = ListPlot [data2, AxesLabel → {"MF ", "AF"},
   PlotStyle → PointSize [0.017 ], DisplayFunction → Identity ];
 p4 = ListPlot [B, PlotLabel → "Molecular fraction ",
   PlotStyle → PointSize [0.017 ], DisplayFunction → Identity ];
 data3 = Table [{q3[[1, i]], q1[[1, i]]}, {i, 1, Nw / NN}];
 CC = Table [{i, q3[[1, i]]}, {i, 1, Nw / NN}];
 p5 = ListPlot [data3, AxesLabel → {"SF ", "AF"},
   PlotStyle → PointSize [0.017 ], PlotStyle → PointSize [0.015 ],
   DisplayFunction → Identity ];
 p6 = ListPlot [CC, PlotLabel → "Stellar fraction ",
   PlotStyle → PointSize [0.017 ], DisplayFunction → Identity ];
 Show [GraphicsArray [{{p1, p2}}], DisplayFunction → $DisplayFunction ];
  Show [GraphicsArray [{{p3, p4}}], DisplayFunction → $DisplayFunction ];
 Show [GraphicsArray [{{p5, p6}}], DisplayFunction → $DisplayFunction ]]
```

Conclusion

The outcomes are addressed. We start with a cosmic subsystem with high heavenly mass part of 0.75. These stars all develop together to a latent state, implying that their masses are recovered in the framework as nuclear gas. To this end the nuclear substance increments pointedly to start with . This nuclear gas is then changed totally into sub-atomic gas, an interaction noticeable as the corner to corner decline on the second of.At last, the framework develops after a few immediately damped motions towards a fixed state with mass part of around 0.40 for the sub-atomic mists, 0.35 for the heavenly substance, and 0.25 for around 5%. The motions are more brutal and this model is portrayed by enormous periods in which the significant piece of the mass is nuclear gas, and practically all the rest atomic. Practically no dynamic stars are available. Then there is a very unexpected change of practically every one of the nuclear gas into sub-atomic gas, quickly followed by an eruption of the star development. Then this multitude of stars develops pretty much, leaving the dynamic star arrangement framework. Their mass is supplanted by new nuclear gas, which turns out to be again the main part.

References

1. K. Maass, V. Geiger, M. R. Ariza, and M. Goos, "The role of mathematics in interdisciplinary STEM education," *ZDM*, vol. 51, no. 6, pp. 869–884, 2019.
2. H. Tian, T. Wang, Y. Liu, X. Qiao, and Y. Li, "Computer vision technology in agricultural automation -- a review," *Information Processing in Agriculture*, vol. 7, no. 1, pp. 1–19, 2020.
3. N. P. Jewell, J. A. Lewnard, and B. L. Jewell, "Predictive mathematical models of the COVID-19 pandemic," *JAMA*, vol. 323, no. 19, pp. 1893-1894, 2020.
4. Y. Qi, "Mathematical expression and application of Marxism," *Applied Mathematics and Nonlinear Sciences*, vol. 6, no. 2, pp. 543–552, 2021.
5. X. Huo, S. Yang, B. Lian, T. Sun, and Y. Song, "A survey of mathematical tools in topology and performance integrated modeling and design of robotic mechanism," *Chinese Journal of Mechanical Engineering*, vol. 33, no. 1, pp. 1–15, 2020.
6. J. A. Nieto, C. C. Nieto-Marín, N. Nieto-Marín, and I. Nieto-Marín, "New mathematical tools for the study of the DNA structure," *Journal of Applied Mathematics and Physics*, vol. 9, no. 8, pp. 1896–1903, 2021.
7. Y. M. Upadhyaya, "Mathematical analysis in static equilibrium of economics: as support to microeconomics course," *Interdisciplinary Journal of Management and Social*
8. D. Kim, D. Jeong, and Y. Seo, "Intelligent design for simulation models of weapon systems using a mathematical structure and case-based reasoning," *Applied Sciences*, vol. 10, no. 21, p. 7642, 2020.
9. J. Liu, M. Yang, E. Tian, J. Cao, and S. Fei, "Event-based security control for state-dependent uncertain systems under hybrid-attacks and its application to electronic circuits," *IEEE Transactions on Circuits and Systems I: Regular Papers*, vol. 66, no. 12, pp. 4817–4828, 2019.
10. F. Arena, G. Pau, and A. Severino, "An overview on the current status and future perspectives of smart cars," *Infrastructures*, vol. 5, no. 7, p. 53, 2020.
11. H. Zhou, W. Xu, J. Chen, and W. Wang, "Evolutionary V2X technologies toward the internet of vehicles: challenges and opportunities," *Proceedings of the IEEE*, vol. 108, no. 2, pp. 308–323, 2020.

12. L. Zhao, J. Yang, S. Wang, and Z. Wu, "Investigation of glass transition behavior in a rice kernel drying process by mathematical modeling," *Drying Technology*, vol. 38, no. 8, pp. 1092–1105, 2020.
13. D. Zhou, X. Du, K. T. Hau, H. Luo, P. Feng, and J. Liu, "Teacher-student relationship and mathematical problem-solving ability: mediating roles of self-efficacy and mathematical anxiety," *Educational Psychology*, vol. 40, no. 4, pp. 473–489, 2020.
14. L. Liang, H. Ye, and G. Y. Li, "Toward intelligent vehicular networks: a machine learning framework," *IEEE Internet of Things Journal*, vol. 6, no. 1, pp. 124–135, 2019.
15. Y. He, S. Yang, C. Y. Chan, L. Chen, and C. Wu, "Visualization analysis of intelligent vehicles research field based on mapping knowledge domain," *IEEE Transactions on Intelligent Transportation Systems*, vol. 22, no. 9, pp. 5721–5736, 2021.
16. F. Granda, L. Azpilicueta, C. Vargas-Rosales et al., "Deterministic propagation modeling for intelligent vehicle communication in smart cities," *Sensors*, vol. 18, no. 7, p. 2133, 2018.
17. H. C. Huang and S. K. Lin, "A hybrid metaheuristic embedded system for intelligent vehicles using hypermutated firefly algorithm optimized radial basis function neural network," *IEEE Transactions on Industrial Informatics*, vol. 15, no. 2, pp. 1062–1069, 2018.
18. X. H. Chang, Y. Liu, and M. Shen, "Resilient control design for lateral motion regulation of intelligent vehicle," *IEEE/ASME Transactions on Mechatronics*, vol. 24, no. 6, pp. 2488–2497, 2019.
19. I. Rasheed, F. Hu, Y. K. Hong, and B. Balasubramanian, "Intelligent vehicle network routing with adaptive 3D beam alignment for mmWave 5G-based V2X communications," *IEEE Transactions on Intelligent Transportation Systems*, vol. 22, no. 5, pp. 2706–2718, 2021.
20. C. Celes, A. Boukerche, and A. A. F. Loureiro, "Mobility trace analysis for intelligent vehicular networks," *ACM Computing Surveys*, vol. 54, no. 3, pp. 1–38, 2022.